SEDIMENTOLOGY the journal of the International Association of Sedimentologists

Sedimentology (2023) **70**, 1281–1301 doi: 10.1111/sed.13077

Controls on grain-size distribution in an ancient sand sea

GABRIEL BERTOLINI*, ADRIAN J. HARTLEY†, JULIANA C. MARQUES* and JHENIFER C. PAIM*

**Instituto de Geociências, Universidade Federal do Rio Grande do Sul, Porto Alegre, 90040-060, Brazil (E-mail: gabertol@gmail.com)*

†Department of Geology & Geophysics, School of Geosciences, University of Aberdeen, Meston Building Room 110, Aberdeen, AB24 3UE, UK

Assosiate Editor – Subhasish Dey

ABSTRACT

Grain-size distribution in deserts is driven by a combination of autogenic controls such as grain abrasion and sorting due to wind transport, and allogenic controls such as provenance and spatial changes in wind-direction. Downwind grain-size trends in present day sand seas display contrasting results, with some showing broad downwind fining and sorting (for example, Namib and Hexi) whilst others lack any clear trend (for example, Ténére, Australian and Sinai). To determine the relative importance of autogenic and allogenic controls on grain-size distribution in sand seas, this study examines the grain-size distribution along the margins of the Cretaceous Botucatu palaeodesert across an area of >1 000 000 km^2. To quantify the main controls on Botucatu palaeodesert grain-size distribution, this study compares the spatial distribution of grain-size metrics with: (i) detrital zircon geochronology as a provenance test; (ii) palaeowind patterns as a wind-regime test; and (iii) three transects along the basin palaeomargins as a downwind abrasion test. Grain-size dispersion shows an east to west fining pattern, which agrees with provenance control – in contrast to a north–south trend expected for the predominant wind-regime control. In the north-east region there is good evidence for downwind fining due to aeolian abrasion – of about 0.4 μm by kilometre, indicating that whilst downwind fining due to abrasion does occur, it is limited by the rounded nature of the available sand and possibly by a mix of different provenance sources. The results suggest that the provenance of the available sand is the primary control on the grain-size distribution in the Botucatu sand sea and potentially in most large-scale dune fields.

Keywords Allogenic controls, autogenic controls, Botucatu, grain-size distribution, palaeoergs, sand seas.

INTRODUCTION

The construction of dune fields by aeolian systems is ruled by a set of external (allogenic) and internal (autogenic) forces. Autogenic forces account for the granular self-organization tendency within natural sedimentary systems (Werner, 1995, 1999; Kocurek & Ewing, 2005). Allogenic controls correspond to external environmental drivers that are linked to external forces such as tectonism, climate or base-level changes (Jerolmack & Paola, 2010; Rodríguez-López *et al.*, 2014). Jerolmack *et al.* (2011) propose that grain-size distributions in aeolian environments are derived from coupled sorting and abrasion due to the saltation of grains in the downwind direction. Abrasion during transport is inherent to the aeolian system (Bagnold, 1941;

Kuenen, 1960; Bullard *et al.*, 2004; Durian *et al.*, 2006), suggesting an autogenic control on grain-size distribution. However, studies on grain-size distribution in modern sand seas find conflicting patterns (Lancaster, 1981, 1985, 1986; Livingstone *et al.*, 1999; Wang *et al.*, 2003; Langford *et al.*, 2016; Bristow & Livingstone, 2019; Liang *et al.*, 2020; Zhou *et al.*, 2021). For instance, in south-west Namibia (Lancaster, 1989), the White Sands in New Mexico (Jerolmack *et al.*, 2011) and the Hexi Corridor in China (Zhang & Dong, 2015) fining and sorting downwind patterns occur over scales of tens of kilometres. In contrast, in the Kalahari in Namibia (Lancaster, 1986), the Ténére in the Sahara (Warren, 1972), the Gibson Desert in Australia (Buckley, 1989) and the Sinai (Sneh & Weissbrod, 1983) no downwind grain-size patterns were identified in dune fields. Langford *et al.* (2016) found evidence that mixing of sand sources in White Sands provided additional controls on dune-field grain-size distribution in contrast to the simple downwind fining and sorting processes proposed by Jerolmack *et al.* (2011) for the same desert. Among these additional controls, wind-regime and the provenance of the available sands are related to external controls on the grain-size dispersion. In summary, the spatial distribution of grain size within desert sands is a combination of the inherent organization patterns in natural granular systems and the available external conditions.

In the sedimentary literature, there is lack of studies that quantify the role of allogenic and autogenic factors that control grain-size distribution in aeolian strata at a basinal scale (>500 000 km^2). This work aims to address this issue using the Botucatu palaeoerg as a case study. The Botucatu palaeoerg is a large-scale (>1 000 000 km^2) dune-field developed in Western Gondwana during the Early Cretaceous (Scherer, 2000; Scherer & Goldberg, 2007). Two main allogenic factors are hypothesized to influence the development of the Botucatu palaeoerg: (i) wind-direction zoning due to the monsoonal climate in Gondwana (Bigarella & Salamuni, 1961; Bigarella & Oliveira, 1966; Scherer & Goldberg, 2007); and (ii) provenance variation derived from the recycling of underlying strata from the Paraná Basin (Bertolini *et al.*, 2020, 2021). Changes in grain size and sorting in a downwind direction can be related to aeolian abrasion, which is intrinsic to the aeolian system and should therefore represent an autogenic signal. To determine the relative roles of autogenic and allogenic controls on grain-size dispersion in deserts, three independent tests were applied, using multiproxy datasets: (i) spatial distribution of provenance changes using detrital zircon; (ii) spatial distribution of wind directions utilizing palaeocurrent data; and (iii) changes in grain size across a number of transects. The tests are used to check and compare: (i) the directionality; and (ii) the magnitude of each mechanism in influencing grain-size dispersion. Ultimately, the paper aims to develop a model that utilizes the grain-size distribution to test the importance of allogenic factors, represented by the wind-direction and provenance zoning, and autogenic factors, evaluated using downwind changes along transects.

BACKGROUND

Grain-size distribution in deserts

The grain-size distribution in desert sands has been the focus of studies since the seminal work of Bagnold (1941) documented in the 'Physics of Blown Sand and Desert Dunes'. Since the late 1970s, the spatial distribution of grain size within modern deserts has been studied extensively by Lancaster (1981, 1982) who pioneered descriptive granulometry analysis in the south-west Africa Kalahari and Namib dune fields. Later, several deserts were the focus of grain-size studies, such as ergs in: China – Taklimakan, Hexi Corridor, Kumtagh (Wang *et al.*, 2003; Zhang & Dong, 2015; Liang *et al.*, 2020); Africa – Namibia, Kalahari, Sinai, Tenéré (Lancaster, 1981, 1985; Watson, 1986; Livingstone, 1987; Thomas, 1988; Bullard *et al.*, 1997; Livingstone *et al.*, 1999); and Australia – Strzelecki, Simpson (Thomas, 1988; Buckley, 1989). These studies focussed on the grain-size distribution at a range of difference scales: (i) differences in grain size within single dunes; (ii) comparison of grain size between individual regions of different dunes such as crests, flanks, plinth or interdune; and (ii) grain-size changes at kilometre scales across large-scale deserts in a downwind direction.

Overall, there are contrasting findings on grain-size distribution at all scales (Langford *et al.*, 2016; Bristow & Livingstone, 2019). At the dune and dune comparison scale, studies in the Namib, Kalahari, Taklimakan and Australian ergs show that dune crests can be finer (Watson, 1986; Livingstone, 1987), coarser

(Wasson, 1983; Thomas, 1988) or equal in grain size to interdunes (Sneh & Weissbrod, 1983; Livingstone *et al.*, 1999; Wang *et al.*, 2003). At the desert scale (>30 000 km^2) (Wilson, 1973), some studies suggest modifications in grain-size attributes along the sand transport direction. Lancaster (1989) found a decrease in grain size and skewness and an increase in sorting along a south to north trend in the Namib Sand Sea – which corresponds to the overall transport direction (Garzanti *et al.*, 2012). Studies in the Hexi corridor desert also found upwind to downwind fining of mean grain size (Zhang & Dong, 2015). Studies in the Kalahari Desert produced conflicting results, Lancaster (1986) describes finer and better-sorted sands along a north-east/south-west transport trend, whereas Livingstone *et al.* (1999) found no trend in granulometry statistics along a 28 km transect. A similar issue occurs in the White Sands dune field in New Mexico, where Langford *et al.* (2016) found evidence of source mixtures influencing grain-size trends using end-member mixtures, whereas Jerolmack *et al.* (2011) proposed a downwind autogenic abrasion control on the fining and sorting in the dune field. The large-scale ergs of Ténére, Gibson and Sinai (>30 000 km^2) also display negligible to no spatial variations in grain-size distribution (Warren, 1972; Sneh & Weissbrod, 1983; Buckley, 1989). In some cases, the fluvial–aeolian interactions can provoke a mixture of sources. For instance, the Kumtagh Sand Sea in north-west China, displays a relationship between grain-size distribution and fluvial–aeolian processes, in which downwind fining occurs, but also a mixture of upwind and locally-derived sands, produces a mixture of zones controlled by either aeolian or fluvial sands (Liang *et al.*, 2020).

In summary, studies from modern sand seas provide a range of different results in assessing the controls on grain-size distribution within dune-scale and erg-scale desert systems. Thus, the nature of grain-size distribution and its relationship with aeolian transport and sand source is still not well-established.

Botucatu palaeoerg

The Early Cretaceous Botucatu palaeoerg covered an area of up to 1 500 000 km^2 in Western Gondwana (Fig. 1), and is preserved in South America and south-west Africa. The palaeodesert is represented by a vast and thick (up to 120 m) sandstone unit referred to as the Botucatu Formation (Brazil), the Rivera Member (Uruguay) and the Twyfelfontein Formation (Namibia). The unit typically crops out as stacked large cross-stratified sandstones, interpreted to be formed by the superimposition of crescentic and linear dunes in a dry–aeolian system (Scherer, 2000, 2002; Scherer & Goldberg, 2007). Exposures of the Botucatu Formation are largely restricted to the margins of the Paraná Basin as it is covered by extensive volcanic and sedimentary strata of the overlying Serra Geral and Bauru formations (Milani *et al.*, 2007). The age of the formation is constrained at the top by radiometric dates from the synchronous continental flood basalts of the Paraná–Etendeka large igneous province (LIP) that are *ca* 134 Ma in age (Ernesto *et al.*, 1999; Thiede & Vasconcelos, 2010; de Assis Janasi *et al.*, 2011; Pinto *et al.*, 2011; Baksi, 2018). The onset of desert conditions is believed to have occurred in the Early Cretaceous and is also thought to have been relatively short-lived due to the lack of supersurfaces and a decrease in the size of fauna as indicated by the ichnofossil assemblage (Francischini *et al.*, 2015). Correlation between the south American and African units is demonstrated by: (i) U–Pb and Ar–Ar dating on Paraná–Etendeka volcanics that overlie the contact with the Botucatu (see review of Gomes & Vasconcelos, 2021); (ii) volcano-sedimentary interactions as dry-peperites or *in situ* dune preservation by lava extrusion (Jerram *et al.*, 2000a,b; Jerram & Stollhofen, 2002; Petry *et al.*, 2007; Waichel *et al.*, 2007, 2008); and (iii) basin correlations based on sedimentological and palaeontological data (Mountney & Howell, 2000; Scherer, 2000, 2002; Marsh & Milner, 2007; Francischini *et al.*, 2015; Porchetti & Wagensommer, 2015; D'Orazi Porchetti *et al.*, 2018; Peixoto *et al.*, 2020).

Provenance studies show that recycled sands were prevalent along the desert margins, mainly sourced from underlying Paraná Basin strata. In detail, Bertolini *et al.* (2020) suggest that a change in provenance occurred from south-west to south-east in the desert based on provenance proxies. In particular, the Cambrian–Neoproterozoic detrital zircon contribution suggests that in the northern area there was a provenance change from the north-west to north-east (Bertolini *et al.*, 2021). Overall, the Botucatu sands result from intense intrabasinal reworking of underlying Paraná Basin strata (Bertolini *et al.*, 2020, 2021); with evidence for east to west

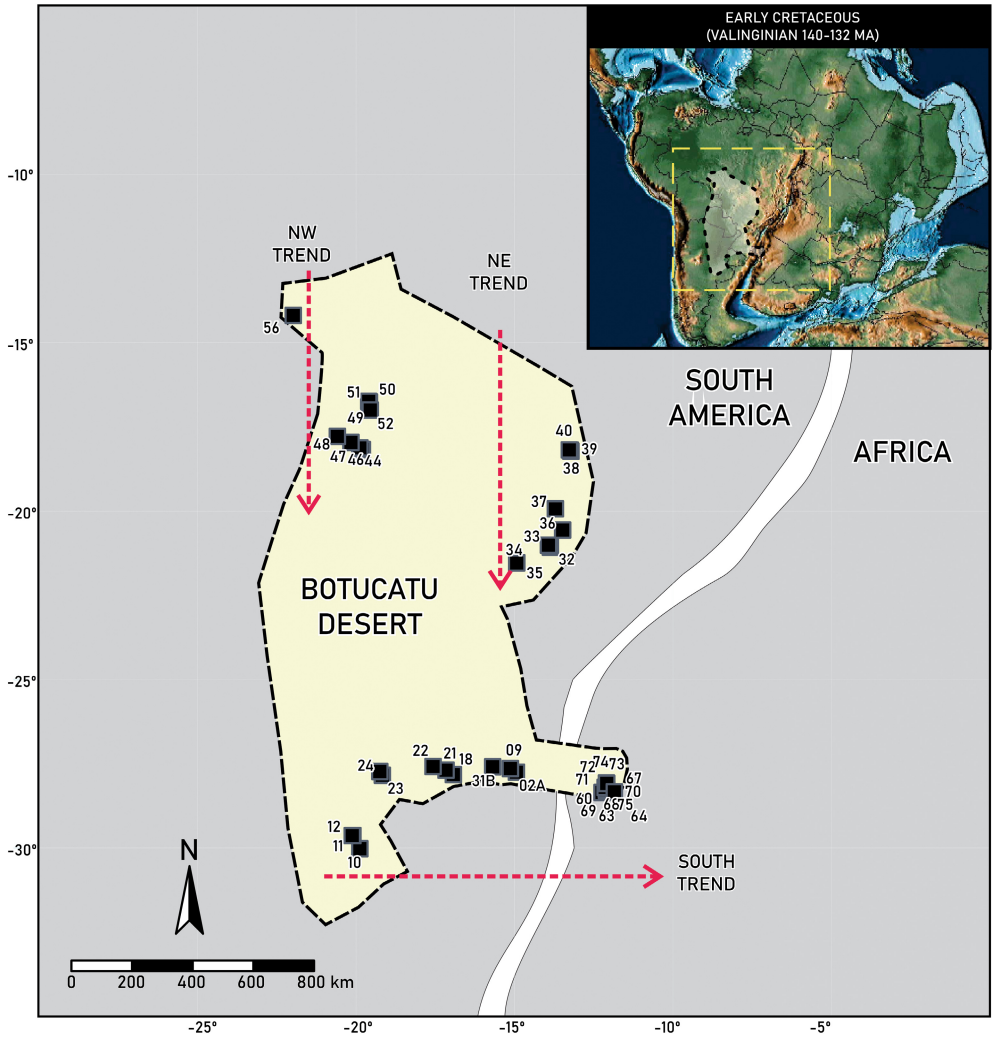

Fig. 1. Grain size sampling sites (Table 1) distributed across three transects (north-west, north-east and south).

shifts in provenance governed by the spatial distribution of the underlying Paraná Basin strata.

METHODOLOGY

This study utilizes 41 sand samples from 39 sites in Brazil, Uruguay and Namibia (Fig. 1). Samples were taken solely from trough cross-stratified sandstones [St(e) facies] to limit sampling bias from different dune locations such as on dune toesets or from aeolian sandsheet deposits. The large-scale trough cross-stratified sandstone sets range from 1 to 20 m in thickness. This facies is interpreted to be formed by sinuous crested dunes comprising mostly grainflow strata, with thinner, finer grained grain-fall laminae and with wind ripple laminae developed at the dune toe on the lee-side (Hunter, 1977; Fryberger & Schenk, 1981). This study presents 12 new samples collected from outcrops in Namibia, in addition to previously published data from South America (Bertolini *et al.*, 2020, 2021). Samples by location, grain-size metrics, wind direction (based on the models from the *Results* section) and literature sources can be found in Appendix S1. Samples were collected over six field trip campaigns between 2015 to 2019, which focussed on the exposed margins of the basin. The central portion of the basin is not sampled because it is covered by extensive volcanics of the Paraná–Etendeka LIP and overlying Cretaceous sedimentary strata. The use of three transects in the

north-east, north-west and south regions are used to display spatially representative profiles of the aeolian system.

Granulometry data were acquired using classical sieving methods for the sand grain size (0.0625 to 2.00 mm) in Centro de Pesquisa Costeira from Universidade Federal do Rio Grande do Sul. Around 100 g of samples were softly disaggregated, to avoid grain breakage, with a rubber pestle and dried in an oven (<100°C). The dry samples then were wet sieved using five grain classes (0, 1, 2, 3, 4 phi). The samples were dried again and individually weighed (Bertolini *et al.*, 2020, 2021). Silt and clay granulometry consists of a mixture of detrital grains and fine cement, so only the sand fraction was selected. Mean grain size, sorting, skewness and kurtosis have been calculated using geometric method of moments by Folk & Ward (1957), using the R package G2Sd (Fournier *et al.*, 2014) which is an R implementation of the Gradistat spreadsheet (Blott & Pye, 2001) for granulometry calculation.

The main uncertainties associated with the dataset include: (i) laminae type (grain-flow, grain-fall and wind-ripples); and (ii) spatial distribution of samples. Sampling was restricted to cross-strata with dip angles >15° and with no obvious visual changes in grain size with the aim of solely sampling grain-flow strata. Previous studies of the Botucatu Formation show that more massive grain-flow strata dominate over millimetre-scale wind-ripple and grain-fall strata (Hunter, 1977; Fryberger & Schenk, 1981; Howell & Mountney, 2001). Thus, whilst sampling of wind ripple and grain-fall strata cannot be ruled out completely, it is believed that sampling in this study is restricted to grain-flow laminae and that the aeolian laminae type is not a significant source of uncertainty.

To mitigate against the lack of exposure in the basin centre resulting from burial by younger strata, specific sampling strategies and applied spatial interpolation techniques were designed. Sampling was done along a series of transects to maximize the spatial distribution of samples around the basin margin and to test hypotheses regarding changes associated with transport and sorting in downwind directions. Spatial interpolation tools were applied to the grain size, provenance and wind-direction data to visualize the behaviour of these attributes. It is recognized that the lack of data in the basin centre introduces significant uncertainty into the interpretation of the interpolated datasets; however, given the large spatial distribution and sampling strategy it is felt that this approach is justified and provides valid results.

The analysis was run in R (R Core Team, 2021) in RStudio Software (https://www.R-project.org/). Data manipulation, wrangling and plots were made using the tidyverse package (Wickham *et al.*, 2019), coordinate transformation to the Early Cretaceous reference frame was undertaken using the chronosphereR package (Kocsis & Raja, 2020), spatial data handling and analysis with SF and SP packages (Pebesma & Bivand, 2005; Pebesma, 2018), interpolation with automap (Hiemstra *et al.*, 2008). The Full code applied here is available at https://github.com/gabertol/controls_grain_size and also as an HTML file in Appendix S2.

RESULTS

The grain-size distribution for dunes from the Botucatu Desert is displayed in Fig. 2. Mean grain size, sorting, kurtosis and skewness were calculated using the geometric method (Folk & Ward, 1957) in millimetres, following the suggestion of Blott & Pye (2001). The dataset displays a mean grain size ranging from 1.05 to 0.05 mm (mean 0.3 mm), sorting from 2.12 to 1.45 (mean 1.68 μm), skewness from 0.57 to −0.35 (mean −0.11 μm) and kurtosis from 1.56 to 0.74 (mean 0.99 μm). Overall, the sands are medium-grained, moderately sorted, mesokurtic and symmetrical to fine skewed.

In detail, the granulometry displays differences based on spatial patterns. Figure 3 displays probability functions from sands from the north and south of the desert, based on the wind model (see *Wind-direction test* section and Fig. 3). The mean grain size, sorting and skewness (Fig. 4A to C) shows different averages from south to north. The north Botucatu area records fine-sands (mean 0.23 mm), moderately well-sorted (mean 1.60 mm) and symmetrically skewed (mean −0.09 mm). The south Botucatu sands are medium (mean 0.35 mm), moderately sorted (mean 1.73 μm) and fine-skewed (mean −0.12 μm). Overall, the southern Botucatu material has coarser and more poorly sorted sands and, consequently, is positively skewed.

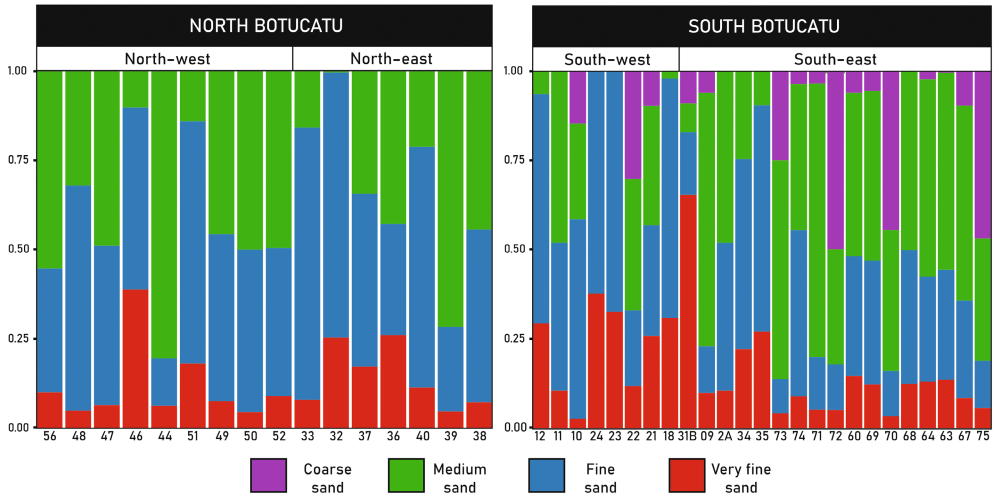

Fig. 2. Grain-size distribution and wind-direction for Botucatu desert samples. Samples ordered from west to east.

Figure 3 shows the changes in granulometry based on region such that spatial changes may be assessed through interpolation. The grain-size metrics have been interpolated with the ordinary kriging method (Fig. 4). The mean grain size (Fig. 4A) shows a dominant trend of coarser sand from south-west/north-east, from 0.38 to 0.10 mm. The south-west region which is located in south-east Brazil and Namibia, comprises the coarsest sands in the desert. Kurtosis, skewness and sorting (Fig. 4B to D) show minor trends – from 50 to 100 km, where high kurtosis, low skewness and low sorting overlap. Overall, the sands are medium in size, moderately sorted, mesokurtic and symmetrical to fine skewed.

The analysis reveals trends in granulometry metrics, in particular the mean grain size. To test the influence of the hypothetical allogenic and autogenic mechanisms on grain-size spatial distribution, three independent tests have been set up. The wind-direction test, provenance test and downwind trend test are used to evaluate respectively the allogenic (wind-regime and the sand-sources) and autogenic (downwind abrasion) forces. The wind-direction test is used to model the wind spatial distribution and classify the predominant wind direction for each granulometry sample. The provenance test aims to model the spatial distribution of sand sources using detrital zircon analyses from 21 samples. The downwind trend test presents linear models for downwind mean grain-size changes across three trends (north-east, north-west and south transects) to check the abrasion along wind transport.

Wind-direction test

Studies of the Botucatu desert show that it records a complex wind pattern (Bigarella & Salamuni, 1961; Bigarella & Oliveira, 1966; Bigarella & Van Eeden, 1970; Scherer, 2000; Scherer & Goldberg, 2007). Three main zones of prevalent wind-direction are documented: a North, South and a mixed zone. The North Botucatu zone is located from 12°S to 20°S (present day latitudes) with a mean wind direction of 213.0°. The South Botucatu wind-zone occurs between 33°S to 25°S (present day latitudes), and a mean direction of 80.2°. The mixed zone is located in the central Botucatu (12°S to 20°S) with polymodal wind directions, presenting a mixture of wind-directions typical for north and south deserts. To evaluate the prevailing wind direction across the desert in order to compare with the grain-size data, palaeocurrents were interpolated from published work (Bigarella & Salamuni, 1961; Bigarella & Oliveira, 1966; Bigarella & Van Eeden, 1970; Mountney & Howell, 2000; Scherer, 2000; Silva & Scherer, 2000; Scherer & Lavina, 2006). Wind direction vector directions from 49 sites were compiled and modelled using the inverse distance weighted algorithm. Figure 5A displays the inverse distance weighted model for the Lower Cretaceous

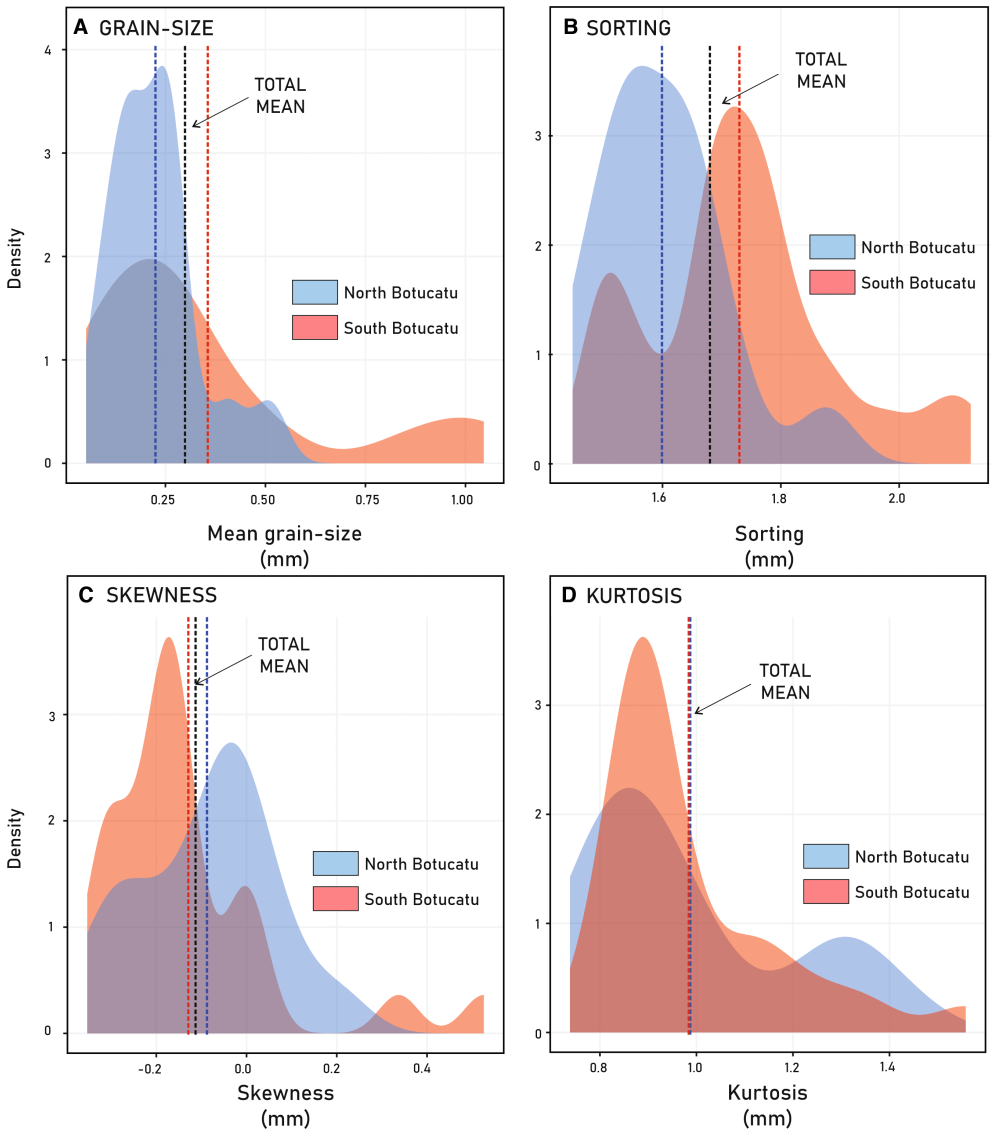

Fig. 3. Grain-size metrics probability density functions illustrating the dunes from the north and south of the Botucatu palaeodesert. Red and blue dashed lines represent south and north Botucatu, respectively. (A) Mean grain size. (B) Sorting. (C) Skewness. (D) Kurtosis.

Gondwana wind direction and a histogram with the distribution of the direction. Appendix S1 files compile the site locations, mean direction, the confidence interval and sources. The mean vector directions and confidence intervals follow the equations of Scherer & Goldberg (2007).

The North Botucatu area registers mean winds blowing to the south/south-west, and the South Botucatu shows prevailing winds blowing towards the north-east. In terms of mode, the wind directions are 80° and 213°. The zone from 20°S to 25°S shows a mixture from both dominant winds, but mostly from northern winds. The model agrees with previous palaeowind studies for the Botucatu Desert (Scherer & Goldberg, 2007) and global circulation models (Moore *et al.*, 1992) that display a monsoon bimodal wind pattern over West Gondwana.

Provenance test

The Botucatu palaeoerg has been the focus of several detrital zircon U–Pb dating studies (Canile *et al.*, 2016; Bertolini *et al.*, 2020, 2021).

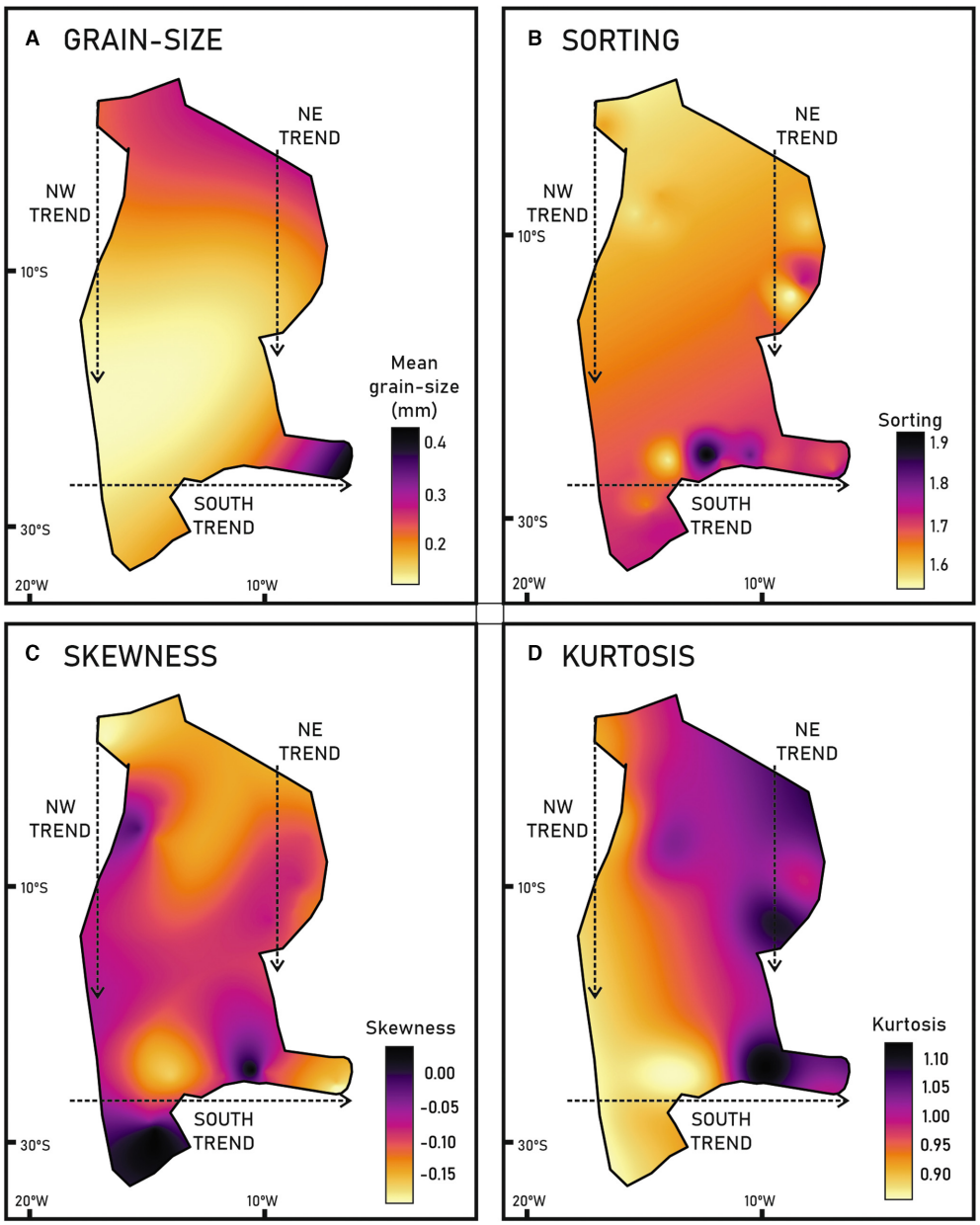

Fig. 4. (A) Mean grain size (mm). (B) Sorting. (C) Skewness. (D) Kurtosis ordinary kriege models.

In this study, 3975 U–Pb detrital ages from 44 samples from Brazil, Uruguay, Argentina and Namibia were compiled. The detrital zircon studies have polymodal distributions, so an appropriate form of representation of their relationships are made using dimensional reduction techniques. An approach widely applied in sedimentary provenance studies, is to use multidimensional scaling plots (Vermeesch, 2013; Vermeesch & Garzanti, 2015). Dimensions 1 and 2 are the most significant, such that a ratio of them simplifies the results into a single proxy. Figure 5B displays the ordinary krieged interpolation with the provenance proxy, indicating a west to east trend in the desert provenance. This agrees with previous provenance studies, that found west–east trends in the provenance of the southern Botucatu Desert – mostly related to changes in the composition of the material in the underlying Paraná Basin strata.

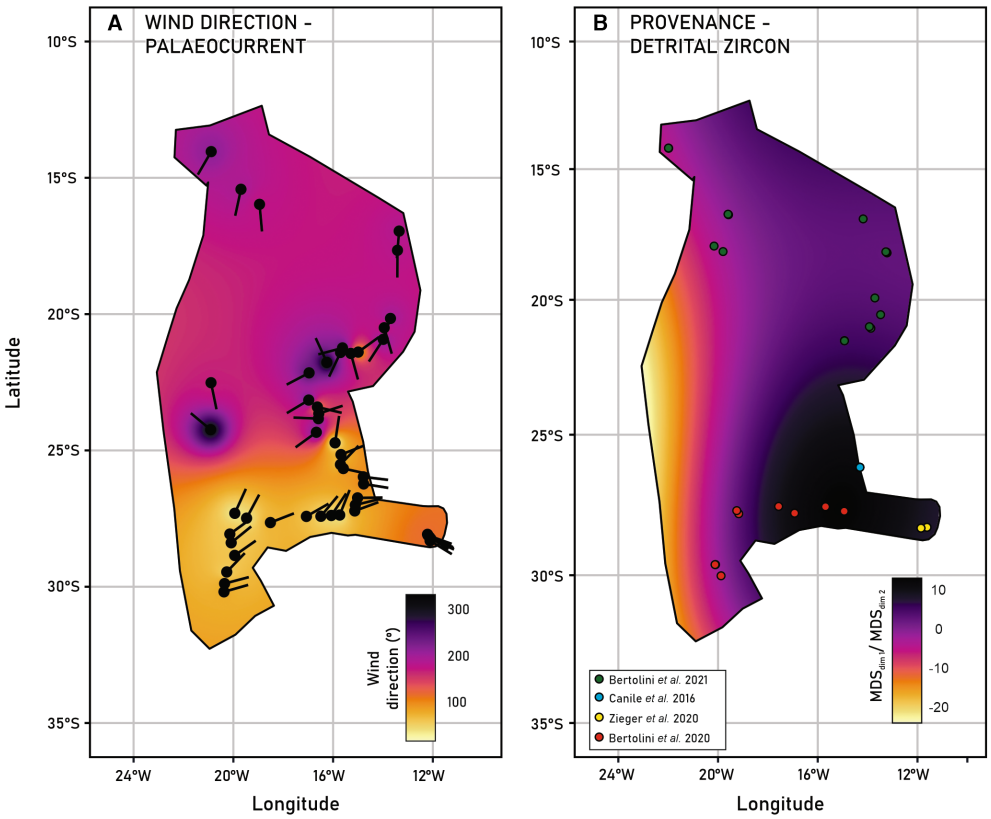

Fig. 5. (A) Inverse distance weight model for Botucatu desert wind-directions. The wind direction distributions show a dominant 80.2° wind in south Botucatu and 213° in north Botucatu. (B) Ordinary kriege interpolation of provenance, using detrital zircon dataset from Canile *et al.* (2016), Bertolini *et al.* (2020, 2021), Zieger *et al.* (2020). The plotted values are a ratio of dimensions 1 and 2 of multidimensional scaling plot.

Downwind trend test

To evaluate the role of wind direction in controlling grain-size distribution, mean grain size was plotted along three transects: north-west, north-east and south (Fig. 6). The transect locations are shown in Fig. 1. The trends vary over hundreds of kilometres. The longitudinal trends correspond to west to east distances, which are equivalent to upwind to downwind due the prevalent north-east wind in the southern region. The latitude trends in the north region (north-east and north-west trends) correspond to north to south distances – equivalent to upwind to downwind in the northern Botucatu zone.

The north-east transect (Fig. 6A) displays a trend of grain-size fining related to palaeolatitude changes in a downwind direction. In the north-west region (Fig. 6B), there is no apparent relationship between latitude and grain size. Lastly, the southern region (Fig. 6C) shows coarser sand towards the west, indicating an upwind fining trend. Linear models and statistics for each model are plotted in Fig. 6.

DISCUSSION

Grain-size distribution of the Botucatu and present-day large-scale ergs

The overall grain-size distribution of the Early Cretaceous Botucatu desert comprises fine to medium, moderately sorted, symmetrical to fine skewed and mesokurtic sands (Figs 2 and 3). The spatial grain-size distribution shows coarser sand overall along the eastern margin (Fig. 3A), while sorting, kurtosis and skewness distribution is constrained to local changes. The wind-direction model (Fig. 5B) shows that in the North and South Botucatu zones, contrasting wind-directions, blowing towards 174° and 73°, respectively, occur. The central region of the desert

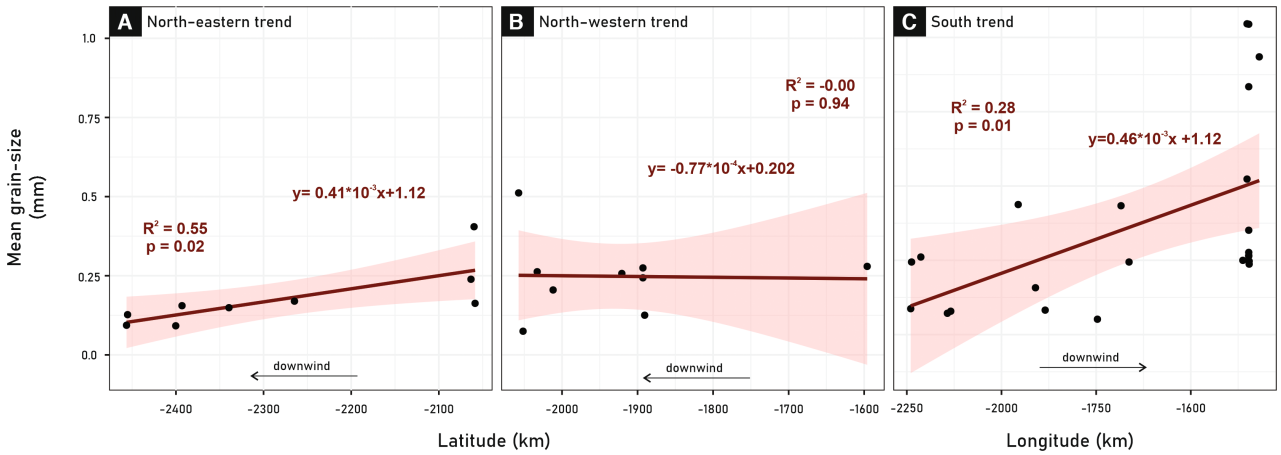

Fig. 6. (A) to (C) Models for mean granulometry along regional transects across palaeolatitude and palaeolongitude distances. Pale-pink area represents standard error.

displays a mixture of both northerly and southerly directed winds, with southerlies predominating. The provenance test (Fig. 5A) shows an east–west trend, in agreement with Bertolini *et al.* (2020) that describes significant changes in detrital zircon and petrographic patterns along a west to east trend in southern Brazil.

In detail, the mean grain-size variation was modelled in a downwind direction in the three transects. The distribution in the north-east transect is explained by a simple linear model (Fig. 6A), which finds P = 0.02 and R^2 of 0.55. The model indicates a fining of 0.0004 mm per kilometre in mean grain size. There is no relationship between grain size and downwind distance in the north-west region, as the model in Fig. 6B shows. Along the southern transect a coarsening trend in a downwind direction is observed. The model (Fig. 6) finds a linear relationship with P = 0.01 and R^2 of 0.28, with a coarsening of 0.46 μm in mean grain size per kilometre. Bigarella (1979) described fining and sorted trends in sands from the north-east Botucatu area, with mean grain size from 2.03 to 1.78 mm and Trask sorting coefficients from 1.44 to 1.32 (Minas Gerais to Paraná states from Brazil). Also, Bigarella (1979) described finer and sorted sands from Rio Grande do Sul to Santa Catarina states (south–north trend in southern Botucatu), with grain size trending from 2.33 to 2.15 mm and Trask sorting from 1.46 to 1.39. The fining trend registered in the north-east region of the Botucatu by Bigarella (1979) is consistent with trends in the present study (Fig. 6A), whilst the southern fining trend is not present in the dataset. However, uncertainties associated with the sampling methodology of Bigarella (1979) mean that it is not possible to undertake a detailed comparison with our datasets.

Table 1 compiles the granulometry statistics for several modern deserts, including the dune types, the sampling position and whether there are any spatial changes within transects. The mean grain size found for the Botucatu is coarser than that documented in modern deserts, such as the south-west Kalahari (Lancaster, 1986), Namib (Lancaster, 1981), Libya (Ahlbrandt, 1979), Simpson (Folk, 1971), Thar (Goudie *et al.*, 1973) and Sinai (Tsoar, 1978). Additionally, the Botucatu is more poorly sorted than other deserts. The mean grain size compared to other deserts is relatively similar, as Table 1 shows that grain size in deserts tends to be centred around 2 phi – corresponding to medium to fine sands. The sorting usually has values around 0.5 – considered to be well-sorted to moderately-sorted. The fining trend in the north-eastern region is similar to that found in other deserts, such as the Namib, Kalahari and Hexi Corridor deserts (Lancaster, 1981, 1986; Zhang & Dong, 2015). Other deserts such as the Ténére, Sinai or Australian erg show no spatial grain-size relationship (Warren, 1972; Sneh & Weissbrod, 1983; Buckley, 1989) and this is also seen in the north-western Botucatu region. In addition, downwind coarsening occurs in the southern region. Results from this study indicate the existence of large-scale downwind abrasion in the north-eastern region, however this is not seen elsewhere in the basin. Previous studies (Kuenen, 1960; Bullard *et al.*, 2004; Durian

Table 1. Granulometry metrics for deserts (values in phi).

Desert	Source	Dune type	Sample position	Trends	Mean grain size	Error	Sorting	Error	Skewness	Error	Kurtosis	Error
Botucatu	Bertolini *et al.* (2020, 2021) & this study	Crescentic, linear	Palaeodunes (cross-stratified sandstones)	North-west no trend	2.17	0.11	0.68	0.02	0.09	0.05	0.96	0.08
		Crescentic, linear		North-east downwind trend in grain-size	2.36	0.1	0.69	0.04	0.08	0.05	1.04	0.06
		Crescentic, linear		South downwind coarsening	2.03	0.11	0.79	0.03	0.14	0.04	0.98	0.04
South-west Kalahari	Lancaster (1986)	Linear dune	Crest	Downwind fining and sorting	2.16	0.2	0.49	0.12	0.14	0.09	0.52	0.03
			North-east flank		2.21	0.19	0.62	0.16	0.05	0.12	0.52	0.02
			South-west flank		2.26	0.18	0.59	0.15	0.07	0.09	0.53	0.04
Namib	Lancaster (1981)	Linear dune	Crest	Dune facies changes - finer and sorted crest than plinth	2.44	0.15	0.37	0.1	0.17	0.13	0.54	0.04
			Base slip face		2.49	0.13	0.34	0.1	0.03	0.12	0.52	0.05
			Mid slip face		2.32	0.14	0.4	0.11	0.05	0.18	0.52	0.04
			Upper west slope		2.41	0.09	0.5	0.09	0.11	0.12	0.5	0.02
			East plinth		2.08	0.16	0.63	0.09	0.2	0.24	0.49	0.08
			West plinth		2.07	0.17	0.75	0.12	0.35	0.18	0.46	0.05
Skeleton Coast	Lancaster (1982)	Transverse and barchan ridges and barchanoids	Crest	Changes in dune types, facies and regional fining and sorting	2.02	0.25	0.51	0.26	0.28	0.19	0.5	0.05
Lybia	Ahlbrandt (1979)	Linear dune	Crest		2.37		0.46					
Canning Basin	Ahlbrandt (1979)	Linear dune	Crest		2.02		0.53					
Simpson Desert	Folk (1971) Wasson (1983)	Linear dune	Crest		2.53		0.43					
					1.62		0.3					
					2.9		0.81					
Thar Desert	Goudie *et al.* (1973)	Linear dune	Crest		2.65		0.56					
Sinai	Tsoar (1978)	Linear dune	Crest		1.87		0.44					

Table 1. (continued)

Desert	Source	Dune type	Sample position	Trends	Mean grain size	Error	Sorting	Error	Skewness	Error	Kurtosis	Error
Yarlung Zangbo	Zhou *et al.* (2021)	Barchans, transverse dunes, crescentic ridges and compound crescetic dunes	Dune		2.12	0.26	0.61	0.18	0.04	0.07	0.97	0.05
Algodones	Sweet *et al.* (1988)	Linear dunes Transverse dunes Draas	Crest Crest Crest		2.49 2.53 2.49		0.37 0.39 0.34					
Kumtagh Sand Sea	Liang *et al.* (2020)	Linear dunes and compound (mega) star dunes	Crest	Downwind fining/ no sorting	2.9 to 1.6		0.8 to 0.2					
El Vizcaíno Desert	Kasper-Zubillaga *et al.* (2007)	Transverse Barchan Transverse and barchan	Crest Crest Crest		2.59 2.59 2.59	0.03 0.03 0.02	0.45 0.43 0.44	0.04 0.02 0.02	0.06 −0.02 0.02	0.01 0.03 0.02	1.05 1.04 1.05	0.04 0.04 0.03
White Sands	Langford *et al.* (2016)	Crescentic ridges, barcanoid and barchan, parabolic	Dunes and interdunes	Downwind sorting and minor fining	2.59 to 0.44 1.06		0.45 to 1.2					

et al., 2006, 2007) show that downwind abrasion should be expected, so additional controls must be acting on the north-western and southern regions. Langford *et al.* (2016) suggested the existence of a mixture of sand sources in the White Dunes desert, interrupting and negating a long-distance trend of sand fining due to wind abrasion. From this perspective, the north-west Botucatu may record a greater mixing of sand sources than seen in the north-east transect.

Allogenic and autogenic controls in grain-size distribution of Botucatu palaeoerg

Dune fields develop under allogenic (environmental factors) and autogenic (self-organization) conditions. In the aeolian realm, the autogenic process is exemplified by dune interactions, deformation during migration, scour of the substrate, or grain-size selection/abrasion (Lancaster, 1981, 1986; Coleman & Melville, 1996; Bridge & Best, 1997; Werner, 1999; Ewing *et al.*, 2015; Pedersen *et al.*, 2015; Zhang & Dong, 2015; Gao *et al.*, 2015a; Swanson *et al.*, 2016, 2019; Cardenas *et al.*, 2019). Allogenic factors relate to the water-table rise/fall, wind and transport direction, source of sand and sand availability (Rubin & Hunter, 1987; Crabaugh & Kocurek, 1993; du Pont *et al.*, 2014; Ping *et al.*, 2014; Ewing *et al.*, 2015; Gao *et al.*, 2015b; Swanson *et al.*, 2017). Allogenic factors are controlled, ultimately, by basin-scale tectonism, climate and base-level changes (Jerolmack & Paola, 2010; Rodríguez-López *et al.*, 2014). Within the Botucatu palaeoerg, the: (i) bimodal wind-direction; and (ii) provenance sources are external forces, so correspond to allogenic variables; whilst (iii) downwind effects are effectively self-organizing and correspond to an autogenic process.

The wind model (Fig. 3) displays two end-member zones of different wind regimes controlled by global circulation patterns and the monsoonal climate (Moore *et al.*, 1992; Scherer & Goldberg, 2007). Grain-size statistics (Fig. 3) show differences from north to south within the different wind regions. At first glance, these may represent a wind-direction control on the Botucatu palaeoerg grain-size distribution; however, apart from the south-west samples, both the northern and southern regions have very similar mean grain size and grain-size metrics (Fig. 2). In contrast, provenance appears to have played an essential role in Botucatu palaeoerg grain-size dispersion, considering the overall east–west shift in provenance (Bertolini *et al.*, 2020, 2021). Downwind fining in the north-east region (Fig. 5A) suggests that the autogenic process occurs, which is consistent with previous studies (Bigarella, 1979). However, such an effect is less dominant than the changes in provenance (allogenic), as revealed by downwind coarsening in the south, the lack of downwind fining in the north-west transect, and east–west grain-size trend in the interpolation model (Fig. 5A).

The ordinary kriege model for the basin (Fig. 4) shows a general grain size fining from east to west, ranging from 0.38 to 0.10 mm. This is in contrast to the regional northerly and southerly trending winds illustrating that the wind direction had a limited effect on grain-size distribution. Skewness, sorting and kurtosis interpolation shows local changes within the southern and northern regions. For instance, kurtosis (Fig. 4D) displays a wider distribution (negative kurtosis values) in the extreme north and south-west regions, suggesting minor shifts in sorting – possibly related to autogenic forces. The sorting, skewness and kurtosis interpolation models (Fig. 4B to D) display regional clusters (from 50 to 100 km), which may show that downwind fining may still operate at smaller scales. Previous studies (Livingstone *et al.*, 1999; Jerolmack *et al.*, 2011; Langford *et al.*, 2016) show variations of around 5 to 30 km which is compatible with the clusters found. However, the regional nature of the dataset limits a more local evaluation. The local sources of sand across the Botucatu (Bertolini *et al.*, 2020, 2021), marked by heavy mineral peaks, suggest that locally derived sands were mixed with 'abraded' sands that were already in the aeolian system.

For autogenic processes, grain abrasion by particle–particle or particle–bed shock is experimentally shown to govern sand size and shape during aeolian transport, but only the north-east region displays a downwind fining trend. The 0.4 μm per kilometre downwind fining is one order of magnitude below that documented in the gypsum-sands of the White Sands Dunefield (Langford *et al.*, 2016). Three main reasons are hypothesized for the lower abrasion rates: (i) hardness difference between quartz and gypsum sands; (ii) low angularity of the multicycle sands of the Botucatu; and (iii) scale differences from the 5 to 10 km transects from Jerolmack *et al.* (2011) and Langford *et al.* (2016) compared to the 400 km transect of this study. Due to the open nature of the desert, where sand can be supplied from around the desert margins, sand mixing will limit strong downwind fining patterns. However, the spatial distributions of sorting,

skewness and kurtosis suggest that autogenic processes do occur but at a more local scale.

Previous studies have determined that downwind fining is not always present in sediments transported by aeolian processes in sand seas (Warren, 1972; Sneh & Weissbrod, 1983; Buckley, 1989; Livingstone *et al.*, 1999). Although it should be noted that loess deposits appear to be spatially linked with sand seas (Crouvi *et al.*, 2008, 2010). Loess deposits of coarse silt to very-fine sand, typically occur downwind of major sand seas (review in Crouvi *et al.*, 2010). From an experimental aeolian transport perspective, studies (Durian *et al.*, 2006, 2007; Roth *et al.*, 2011) show that erosion drives grains into a sphere independent of the original shape. However, erosion is a stationary process (Durian *et al.*, 2007), meaning that after a grain reaches a determinate rounding degree, the process loses its effectiveness. Furthermore, experiments on aeolian abrasion (Kuenen, 1960) find a positive correlation of angularity, grain size and surface roughness with aeolian abrasion rates. The experimental results demonstrate that the fining of sands is very dependent on the angularity of the grains, where rounded grains chip harder than very angular sands. Botucatu sands are comprised of multicycle sands – i.e. sands that have been deposited and reworked several times – thus, the sand grains were rounded prior to entering the sand sea. For instance, in the south-west Botucatu region a mean of 9% of angular grains was recorded by Bertolini *et al.* (2020), as such, only 9% of the grains are susceptible to intense spallation. Most Botucatu palaeoerg sands are sub-rounded to sub-angular, agreeing with other deserts (Goudie & Watson, 1981). In such a case, the effects of downwind fining are constrained by the availability of recycled sands from the underlying Paraná Basin sandstones. In summary, the strongly reworked sands available to the Botucatu aeolian system limit regional scale grain-size fining.

Models for Botucatu grain-size controls and implications for grain-size spatial distribution in sand seas

Considering the wind-direction, provenance and downwind trend tests, provenance changes are the most influential control on the spatial distribution of grain size in the Botucatu Desert. However, other controls can be significant such as aeolian abrasion and source composition and can dominate if the provenance of the sand is considered constant along the desert margin. Figure 7A compiles the grain-size metrics, provenance and wind-direction from each transect in a schematic representation of the Botucatu palaeoerg. The southern transect exhibits a downwind grain-size coarsening due to lateral changes in provenance (Fig. 7A). The north-east transect presents a downwind fining consistent with experimental data on aeolian abrasion (Jerolmack *et al.*, 2011). The north-west transect displays a consistent provenance and grain size along the downwind traverse which suggests a mixture of sands supplied from similar source rocks.

The results suggest that when the source material changes upwind, the mean grain size in the dune-field mirrors these changes in source material. The southern Botucatu sands show a concomitant change in dune sand grain size and lateral variation in the composition of underlying strata that sourced recycled sand material into the dune-field (Bertolini *et al.*, 2020). The magnitude of the lateral variation in grain size can be abrupt and large when provenance dominates the spatial grain-size distribution. For aeolian abrasion to control the grain size in the dune-field, the provenance of the sand must remain constant and have a spatially limited source. If this does not occur, then a provenance signature and variability in the source material will dominate over the aeolian abrasion signal. In summary, the south-east to south-west coarsening and the grain-size interpolation map show that provenance controls the granulometry distribution. In contrast, the northern transect displays evidence of mixing of sand sources and aeolian abrasion. Autogenic forces do occur, but their influence appears to be localized and prone to be removed due to mixing of sands from input points distributed along the desert margins. This conclusion is in contrast to the threshold sand sea hypothesis of Jerolmack & Brzinski (2010), which states that: "*predominant grain size in a sand sea represents particles that are not too far above the threshold for entrainment under the dominant wind*". The southern Botucatu displays a downwind coarsening trend which shows that the same dominant wind can potentially carry different sand sizes due to a provenance change. Thus, there is not a single threshold for sand entrainment, but several considering that each provenance zone has its own energy potential rather than a single one for the whole erg. The available sand for the south Botucatu region is derived from erosion of underlying strata which change laterally, which

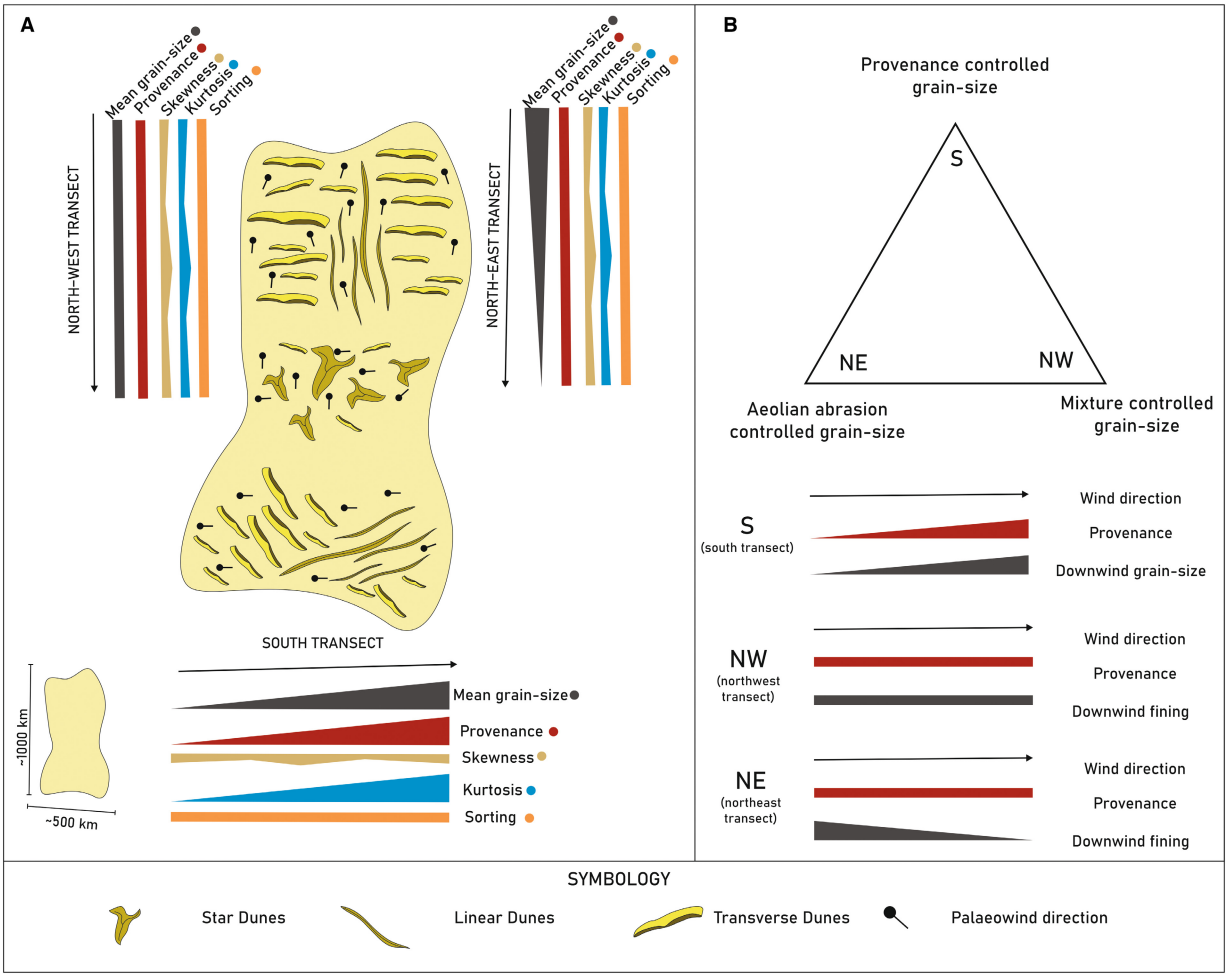

Fig. 7. Models for grain-size distribution along Botucatu palaeoerg margins. (A) Grain-size metrics and provenance along the three transects (south, north-west and north-east) within the Botucatu palaeoerg. (B) End-member process controlling the grain-size dispersion for each region and its characteristics.

is a control that is difficult to incorporate into the threshold sand sea hypothesis. The conundrum is that ultimately the threshold hypothesis implies that the grain size in a sand sea is governed by wind-strength, in some cases, as in the Botucatu desert, however, the wind should be able to carry coarser sands, but the available sand is finer. For a sand sea to be ruled by the threshold hypothesis, the available sand should always be coarser than the threshold grain size for entrainment in the predominant wind. If the entrainment energy of the available sands is lower than the energy of the predominant wind, the provenance changes rule the predominant particle size in a sand sea.

The threshold hypothesis can operate in small-scale deserts such as the White Sands (*ca* 400 km^2) or single-sourced deserts, but for large-scale deserts such as the Botucatu (*ca* 1 000 000 km^2) the number and magnitude of sources and their mixtures across the dominant wind need to be considered. Furthermore, to predict the mixture of sources in sand seas can be difficult due to different geological/geomorphic factors that may be unique to each desert (Rittner *et al.*, 2016; Farrant *et al.*, 2019; Garzanti *et al.*, 2020, 2021; Pastore *et al.*, 2021). An alternative interpretation for the sand sea threshold hypothesis, is to consider that *n* sources of sand within a desert are ruled by the hypothesis individually, while the predominant grain size in a sand sea should be a product of the mixture of these *n* sources after the effects of sorting and fining downwind.

The grain size, provenance and wind-direction distribution of each transect are

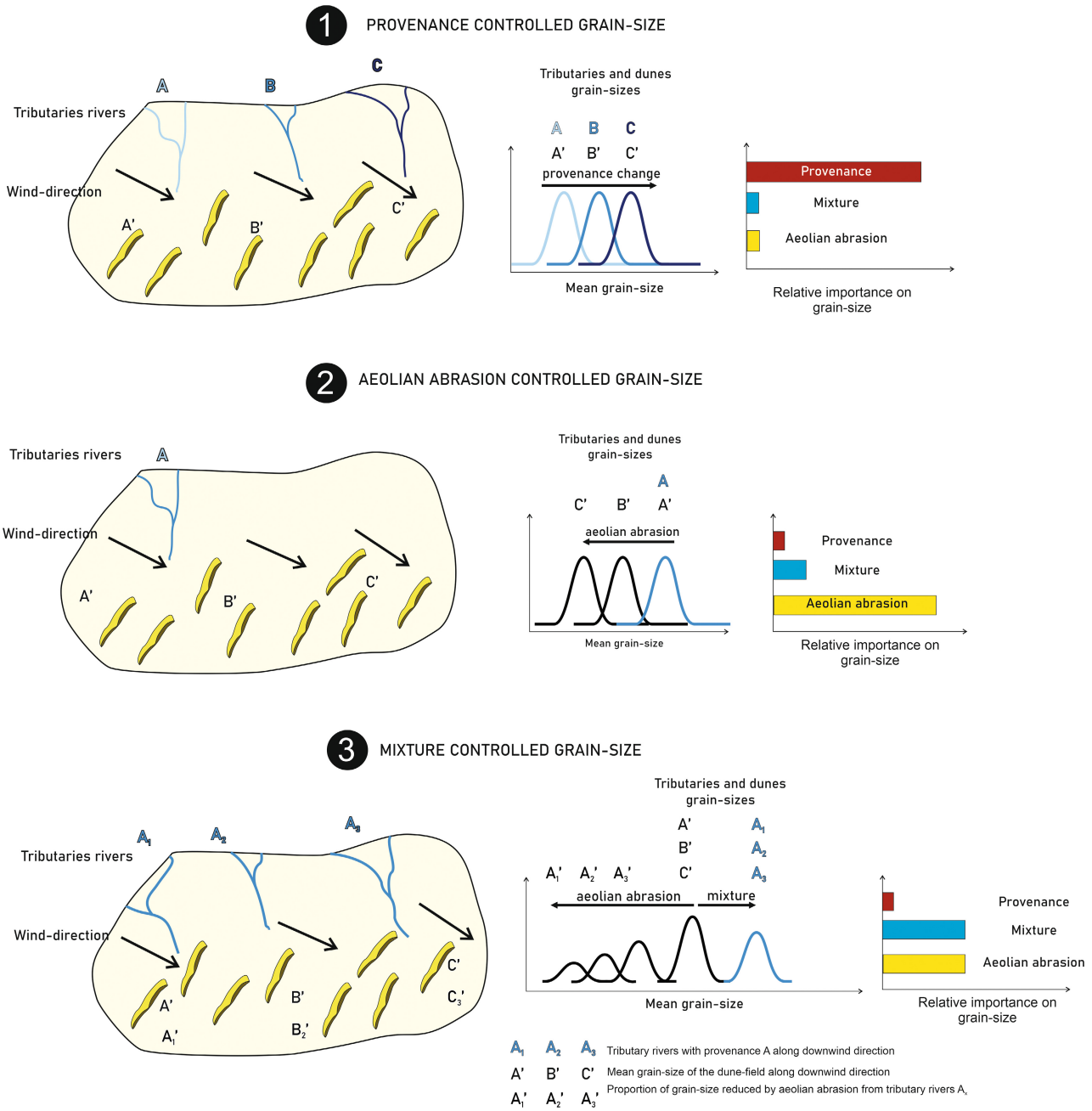

Fig. 8. Models for spatial changes in grain size within dune fields controlled by: (1) provenance; (2) aeolian abrasion; and (3) mixture. The schemes show the relationship of catchment grain size with aeolian abrasion and provenance changes, illustrating dune field schemes and relationships with detrital grain sizes from river catchments.

hypothesized to be controlled by three processes (Fig. 8); provenance (south transect), mixing (north-west transect) and aeolian abrasion (north-east transect). For grain size controlled by provenance, the catchment rivers should display different sources along the downwind direction (Fig. 8). The change in provenance does not necessarily relate to sand sourced from outside the basin but can be related to lateral facies changes or stratigraphic changes within underlying strata. For grain size to be controlled by aeolian abrasion, there must not be any change in provenance within the catchment of the rivers supplying sediment to the basin, and the sands

that are supplied can only have a limited mixture. For the aeolian abrasion model, Fig. 8 proposes that a single catchment sourced the sand upwind of the desert with no mixing of sources in a downwind direction. In this scenario, the spatial distribution of the grain size is explained directly by the magnitude of the aeolian abrasion. The aeolian abrasion is controlled by the desert sand morphology together with the wind-strength and direction. The grain size controlled by mixing occurs when provenance does not change in a downwind direction, but when mixing of the abraded sands that have been transported into the aeolian system through input of 'immature' sands from basin margin rivers overrides the downwind fining. This process records a balance of two opposing controls on: (i) the mean grain size; (ii) the aeolian abrasion decreasing the grain size downwind; and (iii) the input of coarser sands from catchment sources along the downwind direction.

Overall, these autogenic and allogenic controls relate to conditions expected to be universal for aeolian systems. For instance, several ancient aeolian systems register regional changes in wind direction (Parrish & Peterson, 1988; Peterson, 1988; Giannini *et al.*, 2004; Mescolotti *et al.*, 2019; Shozaki & Hasegawa, 2021; Yu *et al.*, 2021a,b), modern deserts display changes in provenance along their margins (Garzanti *et al.*, 2012; Rittner *et al.*, 2016; Pastore *et al.*, 2021), as well as aeolian abrasion that is shown to be observed in both the field (Crouvi *et al.*, 2008, 2010) and experiments (Kuenen, 1960; Bullard *et al.*, 2004; Durian *et al.*, 2006, 2007; Roth *et al.*, 2011). Thus, the provenance, aeolian abrasion, and mixture of these process recorded in the Botucatu palaeodesert are potentially important in aeolian desert systems in general. The predominance of each process relates to specific aspects of each geological context that define features such as variations in provenance, wind regimes and strength, and sand mineralogy and morphologies (for example, angular-rounded or bladded-spheric, quartz-bearing or gypsum-bearing sands).

CONCLUSION

Based on 41 granulometry samples from cross-stratified sandstones of the Botucatu palaeoerg in Brazil, Uruguay and Namibia, this study detailed the spatial distribution of grain size in an ancient large-scale dune field. Furthermore, the study assessed the grain-size distribution with a palaeowind direction model and a provenance model, based on previously published data obtained in sandstone palaeodunes. From these data it can be concluded that:

- Minor to non-existent changes in granulometry are related to zones with different predominant winds.
- Basin-scale grain-size changes were controlled primarily by provenance sources rather than by wind-direction, downwind fining or sorting due abrasion during transport.
- Available recycled sand controls the grain-size distribution.
- Recycled and rounded sands and mixture of sources limits the downwind fining.
- Downwind selection effects are probably limited to local scale, within 50 to 100 km.

ACKNOWLEDGEMENTS

The authors would like to thank Subhasish Dey for editing, Claiton Scherer and an anonymous reviewer for their constructive reviews. We thank Bernardo Peixoto for reviewing the manuscript and palaeocoordinate conversion code debug. We thank several colleagues from the all over the world that joined us during field-trips in Brazil, Uruguay and Namibia.

DATA AVAILABILITY STATEMENT

The data that supports the findings of this study are available in the supplementary material of this article.

REFERENCES

Ahlbrandt, T.S. (1979) Textural parameters of eolian deposits. *Study Glob. Sand Seas Geol. Surv. Prof. Pap.*, **1052**, 429.

de Assis Janasi, V., **de Freitas, V.A.** and **Heaman, L.H.** (2011) The onset of flood basalt volcanism, northern Paraná Basin, Brazil: a precise U-Pb baddeleyite/zircon age for a Chapecó-type dacite. *Earth Planet. Sci. Lett.*, **302**, 147–153.

Bagnold, R.A. (1941) *The Physics of Blown Sand and Desert Dunes*. Methuen, London, 265 pp.

Baksi, A.K. (2018) Paraná flood basalt volcanism primarily limited to ~ 1 Myr beginning at 135 ma: new 40Ar/39Ar ages for rocks from Rio Grande do Sul, and critical evaluation of published radiometric data. *J. Volcanol. Geotherm. Res.*, **355**, 66–77.

Bertolini, G., **Marques, J.C.**, **Hartley, A.J.**, **Da-Rosa, A.A.S.**, **Scherer, C.M.S.**, **Basei, M.A.S.** and **Frantz, J.C.** (2020) Controls on early cretaceous desert sediment provenance in south-West Gondwana, Botucatu formation (Brazil and Uruguay). *Sedimentology*, **67**, 2672–2690.

Bertolini, G., **Marques, J.C.**, **Hartley, A.J.**, **Basei, M.A.S.**, **Frantz, J.C.** and **Santos, P.R.** (2021) Determining sediment provenance history in a Gondwanan erg: Botucatu formation, northern Paraná Basin, Brazil. *Sediment. Geol.*, **417**, 105883.

Bigarella, J. (1979) Botucatu and Sambaiba sandstones of South America (Jurassic and cretaceous); and cave sandstone and similar sandstones of southern Africa (Triassic). *Study Glob. Sand Seas U.S. Geol. Surv. Prof. Pap.*, **1052**, 233–238.

Bigarella, J.J. and **Oliveira, M.A.M.d.** (1966) Nota preliminar sobre as direções de transporte dos arenitos Furnas e Botucatu na parte setentrional da Bacia do Paraná. *Bol. Parana. Geogr.*, **18**, 20.

Bigarella, J.J. and **Salamuni, R.** (1961) Early mesozoic wind patterns as suggested by dune bedding in the botucatú sandstone of Brazil and Uruguay. *Bull. Geol. Soc. Am.*, **72**, 1089–1105.

Bigarella, J.J. and **Van Eeden, O.R.** (1970) Mesozoic palaeowind patterns and the problem of continental drift. *Bol. Parana. Geociências*, **28**, 115–144.

Blott, S.J. and **Pye, K.** (2001) Gradistat: a grain size distribution and statistics package for the analysis of unconsolidated sediments. *Earth Surf. Process. Landf.*, **26**, 1237–1248.

Bridge, J. and **Best, J.** (1997) Preservation of planar laminae due to migration of low-relief bed waves over aggrading upper-stage plane beds: comparison of experimental data with theory. *Sedimentology*, **44**, 253–262.

Bristow, C. and **Livingstone, I.** (2019) Dune sediments. In: *Aeolian Geomorphology: A New Introduction*, pp. 209–236. John Wiley & Sons, Chichester.

Buckley, R. (1989) Grain-size characteristics of linear dunes in Central Australia. *J. Arid Environ.*, **16**, 23–28.

Bullard, J.E., **Thomas, D.S.G.**, **Livingstone, I.** and **Wiggs, G.S.F.** (1997) Dunefield activity and interactions with climatic variability in the Southwest Kalahari Desert. *Earth Surf. Process. Landf.*, **22**, 165–174.

Bullard, J.E., **McTainsh, G.H.** and **Pudmenzky, C.** (2004) Aeolian abrasion and modes of fine particle production from natural red dune sands: an experimental study. *Sedimentology*, **51**, 1103–1125.

Canile, F.M., **Babinski, M.** and **Rocha-Campos, A.C.** (2016) Evolution of the carboniferous-early cretaceous units of Paraná Basin from provenance studies based on U-Pb, Hf and O isotopes from detrital zircons. *Gondw. Res.*, **40**, 142–169.

Cardenas, B.T., **Kocurek, G.**, **Mohrig, D.**, **Swanson, T.**, **Hughes, C.M.** and **Brothers, S.C.** (2019) Preservation of autogenic processes and allogenic Forcings in set-scale Aeolian architecture II: the scour-and-fill dominated Jurassic page sandstone, Arizona, U.S.A. *J. Sediment. Res.*, **89**, 741–760.

Coleman, S. and **Melville, B.** (1996) Initiation of bed forms on a flat sand bed. *J. Hydraul. Eng.*, **122**, 301–310.

Crabaugh, M. and **Kocurek, G.** (1993) Entrada sandstone: an example of a wet aeolian system. *Geol. Soc. Spec. Publ.*, **72**, 103–126.

Crouvi, O., **Amit, R.**, **Enzel, Y.**, **Porat, N.** and **Sandler, A.** (2008) Sand dunes as a major proximal dust source for late Pleistocene loess in the Negev Desert, Israel. *Quat. Res.*, **70**, 275–282.

Crouvi, O., **Amit, R.**, **Enzel, Y.** and **Gillespie, A.R.** (2010) Active sand seas and the formation of desert loess. *Quat. Sci. Rev.*, **29**, 2087–2098.

D'Orazi Porchetti, S., **Bertini, R.J.** and **Langer, M.C.** (2018) Proposal for ichnotaxonomic allocation of therapsid footprints from the Botucatu formation (Brazil). *Ichnos*, **25**, 192–207.

Durian, D.J., **Bideaud, H.**, **Duringer, P.**, **Schröder, A.**, **Thalmann, F.** and **Marques, C.M.** (2006) What is in a pebble shape? *Phys. Rev. Lett.*, **97**, 1–4.

Durian, D.J., **Bideaud, H.**, **Duringer, P.**, **Schröder, A.P.** and **Marques, C.M.** (2007) Shape and erosion of pebbles. *Phys. Rev. E – Stat. Nonlinear Soft Matter Phys.*, **75**, 1–9.

Ernesto, M., **Raposo, M.I.B.**, **Marques, L.S.**, **Renne, P.R.**, **Diogo, L.A.** and **De Min, A.** (1999) Paleomagnetism, geochemistry and 40Ar/39Ar dating of the north-eastern Parana Magmatic Province: tectonic implications. *J. Geodyn.*, **28**, 321–340.

Ewing, R.C., **McDonald, G.D.** and **Hayes, A.G.** (2015) Multi-spatial analysis of aeolian dune-field patterns. *Geomorphology*, **240**, 44–53.

Farrant, A.R., **Mounteney, I.**, **Burton, A.**, **Thomas, R.J.**, **Roberts, N.M.W.**, **Knox, R.W.O.** and **Bide, T.** (2019) Gone with the wind: dune provenance and sediment recycling in the northern rub' al-khali, United Arab Emirates. *J. Geol. Soc. London*, **176**, 269–283.

Folk, R.L. (1971) Longitudinal dunes of the northwestern edge of the Simpson Desert. *Sedimentology*, **16**, 5–54.

Folk, R.L. and **Ward, W.C.** (1957) Brazos River bar [Texas]; a study in the significance of grain size parameters. *J. Sediment. Petrol.*, **27**, 3–26.

Fournier, J., **Gallon, R.K.** and **Paris, R.** (2014) G2Sd: a new R package for the statistical analysis of unconsolidated sediments. *Géomorphol. Relief Proc. Environ.*, **20**, 73–78.

Francischini, H., **Dentzien-Dias, P.C.**, **Fernandes, M.A.** and **Schultz, C.L.** (2015) Dinosaur ichnofauna of the upper Jurassic/lower cretaceous of the Paraná Basin (Brazil and Uruguay). *J. South Am. Earth Sci.*, **63**, 180–190.

Fryberger, S.G. and **Schenk, C.** (1981) Wind sedimentation tunnel experiments on the origins of aeolian strata. *Sedimentology*, **28**, 805–821.

Gao, X., **Narteau, C.** and **Rozier, O.** (2015a) Development and steady states of transverse dunes: a numerical analysis of dune pattern coarsening and giant dunes. *J. Geophys. Res. F Earth Surf.*, **120**, 2200–2219.

Gao, X., **Narteau, C.**, **Rozier, O.** and **Du Pont, S.C.** (2015b) Phase diagrams of dune shape and orientation depending on sand availability. *Sci. Rep.*, **5**, 1–12.

Garzanti, E., **Andò, S.**, **Vezzoli, G.**, **Lustrino, M.**, **Boni, M.** and **Vermeesch, P.** (2012) Petrology of the Namib Sand Sea: long-distance transport and compositional variability in the wind-displaced Orange Delta. *Earth Sci. Rev.*, **112**, 173–189.

Garzanti, E., **Liang, W.**, **Andò, S.**, **Clift, P.D.**, **Resentini, A.**, **Vermeesch, P.** and **Vezzoli, G.** (2020) Provenance of Thal Desert sand: focused erosion in the western Himalayan syntaxis and foreland-basin deposition driven by latest quaternary climate change. *Earth Sci. Rev.*, **207**, 103220.

Garzanti, E., **Pastore, G.**, **Stone, A.**, **Vainer, S.**, **Vermeesch, P.** and **Resentini, A.** (2021) Provenance of Kalahari sand: Paleoweathering and recycling in a linked fluvial-aeolian system. *Earth Sci. Rev.*, **227**, 103867.

Giannini, P.C.F., **Sawakuchi, A.D.O.**, **Fernandes, L.A.** and **Donatti, L.M.** (2004) Paleoventos e paleocorrentes subaquosas do sistema deposicional Pirambóia nos estados de São Paulo e Paraná: Estudo baseado em estatística de dados azimutais. *Rev. Bras. Geociências*, **34**, 282–292.

Gomes, A.S. and **Vasconcelos, P.M.** (2021) Geochronology of the Paraná-Etendeka large igneous province. *Earth Sci. Rev.*, **220**, 103716.

Goudie, A.S. and **Watson, A.** (1981) The shape of desert sand dune grains. *J. Arid Environ.*, **4**, 185–190.

Goudie, A.S., **Allchin, B.** and **Hegde, K.T.M.** (1973) The former extensions of the great Indian Sand Desert author. *R. Geogr. Soc.*, **139**, 243–257.

Hiemstra, P.H., **Pebesma, E.J.**, **Twenhöfel, C.J.W.** and **Heuvelink, G.B.M.** (2008) Real-time automatic interpolation of ambient gamma dose rates from the Dutch radioactivity monitoring network. *Comput. Geosci.*, **35**, 1711–1721.

Howell, J. and **Mountney, N.** (2001) Aeolian grain flow architecture: hard data for reservoir models and implications for red bed sequence stratigraphy. *Pet. Geosci.*, **7**, 51–56.

Hunter, R.E. (1977) Basic types of stratification in small eolian dunes. *Sedimentology*, **24**, 361–387.

Jerolmack, D.J. and **Brzinski, T.A.** (2010) Equivalence of abrupt grain-size transitions in alluvial rivers and eolian sand seas: a hypothesis. *Geology*, **38**, 719–722.

Jerolmack, D.J. and **Paola, C.** (2010) Shredding of environmental signals by sediment transport. *Geophys. Res. Lett.*, **37**, 1–5.

Jerolmack, D.J., **Reitz, M.D.** and **Martin, R.L.** (2011) Sorting out abrasion in a gypsum dune field. *Case Rep. Med.*, **116**, 1–15.

Jerram, D.A. and **Stollhofen, H.** (2002) Lava–sediment interaction in desert settings; are all peperite-like textures the result of magma–water interaction? *J. Volcanol. Geotherm. Res.*, **114**, 231–249.

Jerram, D.A., **Mountney, N.**, **Howell, J.** and **Stollhofen, H.** (2000a) The Fossilised Desert: recent developments in our understanding of the lower cretaceous deposits in the Huab Basin, NW Namibia. *Communs. Geol. Surv. Namibia*, **12**, 303–313.

Jerram, D.A., **Mountney, N.P.**, **Howell, J.A.**, **Long, D.** and **Stollhofen, H.** (2000b) Death of a sand sea: an active aeolian erg systematically buried by the Etendeka flood basalts of NW Namibia. *J. Geol. Soc. London*, **157**, 513–516.

Kasper-Zubillaga, J.J. and **Zolezzi-Ruiz, H.** (2007) Grain size, mineralogical and geochemical studies of coastal and inland dune sands from El Vizcaíno Desert, Baja California Peninsula, Mexico. *Rev Mex Cienc Geol.*, **24**, 423–438.

Kocsis, A.T. and **Raja, N.B.** (2020) chronosphere: Earth system history variables. https://doi.org/10.5281/zenodo.3530703

Kocurek, G. and **Ewing, R.C.** (2005) Aeolian dune field self-organization - implications for the formation of simple versus complex dune-field patterns. *Geomorphology*, **72**, 94–105.

Kuenen, P.H. (1960) Experimental abrasion 4: Eolian action. *J. Geol.*, **68**, 427–449.

Lancaster, N. (1981) Grain size characteristics of Namib Desert linear dunes. *Sedimentology*, **28**, 115–122.

Lancaster, N. (1982) Dunes on the skeleton coast, Namibia (south West Africa): geomorphology and grain size relationships. *Earth Surf. Process. Landf.*, **7**, 575–587.

Lancaster, N. (1985) Winds and sand movements in the Namib Sand Sea. *Earth Surf. Process. Landf.*, **10**, 607–619.

Lancaster, N. (1986) Grain-size characteristics of linear dunes in the southwestern Kalahari. *J. Sediment. Petrol.*, **56**, 395–400.

Lancaster, N. (1989) *The Namib Sand Sea: Dune Forms, Processes and Sediments*. Balkema, Rotterdam.

Langford, R.P., **Gill, T.E.** and **Jones, S.B.** (2016) Transport and mixing of eolian sand from local sources resulting in variations in grain size in a gypsum dune field, White Sands, New Mexico, USA. *Sediment. Geol.*, **333**, 184–197.

Liang, A., **Dong, Z.**, **Qu, J.**, **Su, Z.**, **Wu, B.**, **Zhang, Z.**, **Qian, G.**, **Gao, J.**, **Pang, Y.** and **Yang, Z.** (2020) Using spatial variations of grain size to reveal sediment transport in the Kumtagh Sand Sea, Northwest China. *Aeolian Res.*, **46**, 100599.

Livingstone, I. (1987) Grain-size variation on a "complex" linear dune in the Namib Desert. *Geol. Soc. Spec. Publ.*, **35**, 281–291.

Livingstone, I.A.N., **Bullard, J.E.**, **Wiggs, G.F.S.** and **Thomas, D.S.G.** (1999) Grain-size variation on dunes in the southwest kalahari, southern Africa. *J. Sediment. Res.*, **69**, 546–552.

Marsh, J.S. and **Milner, S.C.** (2007) Stratigraphic correlation of the Awahab and Tafelberg formations, Etendeka group, Namibia, and location of an eruptive site for flood basalt volcanism. *J. Afr. Earth Sci.*, **48**, 329–340.

Mescolotti, P.C., **Varejão, F.G.**, **Warren, L.V.**, **Ladeira, F.S.B.**, **Giannini, P.C.F.** and **Assine, M.L.** (2019) The sedimentary record of wet and dry eolian systems in the cretaceous of Southeast Brazil: stratigraphic and paleogeographic significance, Brazil. *J. Geol.*, **49**, e20190057.

Milani, E.J., **Melo, J.H.G.**, **Souza, P.A.**, **Fernandes, L.A.** and **França, A.B.** (2007) Bacia do Paraná. *Bol Geociências Petrobrás*, **15**, 265–287.

Moore, G.T., **Hayashida, D.N.**, **Ross, C.A.** and **Jacobson, S.R.** (1992) Paleoclimate of the Kimmeridgian/Tithonian (late Jurassic) world: I. results using a general circulation model. *Palaeogeogr. Palaeoclimatol. Palaeoecol.*, **93**, 113–150.

Mountney and Howell (2000) Aeolian architecture, bedform climbing and preservation space in the cretaceous Etjo formation, NW Namibia. *Sedimentology*, **47**, 825–849.

Parrish, J.T. and **Peterson, F.** (1988) Wind directions predicted from global circulation models and wind directions determined from eolian sandstones of the western United States—a comparison. *Sediment. Geol.*, **56**, 261–282.

Pastore, G., **Baird, T.**, **Vermeesch, P.**, **Resentini, A.** and **Garzanti, E.** (2021) Provenance and recycling of Sahara Desert sand. *Earth Sci. Rev.*, **216**, 103606.

Pebesma, E.J. (2018) Simple features for R: standardized support for spatial vector data. *R Journal*, **10**, 439.

Pebesma, E. and **Bivand, R.S.** (2005) S classes and methods for spatial data: the SP package. *R News*, **5**, 9–13.

Pedersen, A., **Kocurek, G.**, **Mohrig, D.** and **Smith, V.** (2015) Dune deformation in a multi-directional wind regime: white sands dune field, New Mexico. *Earth Surf. Process. Landf.*, **40**, 925–941.

Peixoto, B.C.P.M., **Mángano, M.G.**, **Minter, N.J.**, **dos Reis Fernandes, L.B.** and **Fernandes, M.A.** (2020) A new insect trackway from the upper Jurassic—lower cretaceous eolian sandstones of São Paulo state, Brazil: implications for reconstructing desert paleoecology. *PeerJ*, **8**, e8880.

Peterson, F. (1988) Pennsylvanian to Jurassic eolian transportation systems in the western United States. *Sediment. Geol.*, **56**, 207–260.

Petry, K., **Jerram, D.A.**, **de Almeida, D.** and **Zerfass, H.** (2007) Volcanic-sedimentary features in the Serra Geral Fm., Paraná Basin, southern Brazil: examples of dynamic lava-sediment interactions in an arid setting. *J. Volcanol. Geotherm. Res.*, **159**, 313–325.

Ping, L., **Narteau, C.**, **Dong, Z.**, **Zhang, Z.** and **Courrech Du Pont, S.** (2014) Emergence of oblique dunes in a landscape-scale experiment. *Nat. Geosci.*, **7**, 99–103.

Pinto, V.M., **Hartmann, L.A.**, **Santos, J.O.S.**, **McNaughton, N.J.** and **Wildner, W.** (2011) Zircon U-Pb geochronology from the Paraná bimodal volcanic province support a brief eruptive cycle at ~135Ma. *Chem. Geol.*, **281**, 93–102.

du Pont, S.C., **Narteau, C.** and **Gao, X.** (2014) Two modes for dune orientation. *Geology*, **42**, 743–746.

Porchetti, S.D. and **Wagensommer, A.** (2015) A vertebrate trackway from the Twyfelfontein formation (lower cretaceous), Damaraland, Namibia. *Paläontol. Z.*, **89**, 807–814.

R Core Team (2021) *R: A Language and Environment for Statistical Computing*. R Foundation for Statistical Computing, Vienna.

Rittner, M., **Vermeesch, P.**, **Carter, A.**, **Bird, A.**, **Stevens, T.**, **Garzanti, E.**, **Andò, S.**, **Vezzoli, G.**, **Dutt, R.**, **Xu, Z.** and **Lu, H.** (2016) The provenance of Taklamakan Desert sand. *Earth Planet. Sci. Lett.*, **437**, 127–137.

Rodríguez-López, J.P., **Clemmensen, L.B.**, **Lancaster, N.**, **Mountney, N.P.** and **Veiga, G.D.** (2014) Archean to recent aeolian sand systems and their sedimentary record: current understanding and future prospects. *Sedimentology*, **61**, 1487–1534.

Roth, A.E., **Marques, C.M.** and **Durian, D.J.** (2011) Abrasion of flat rotating shapes. *Phys Rev E - Stat Nonlinear Soft Matter Phys.*, **83**, 1–8.

Rubin, D.M. and **Hunter, R.E.** (1987) Bedform alignment in directionally varying flows. *Science*, **237**, 276–278.

Scherer, C.M.S. (2000) Eolian dunes of the Botucatu formation (cretaceous) in southernmost Brazil: morphology and origin. *Sediment. Geol.*, **137**, 63–84.

Scherer, C.M.S. (2002) Preservation of aeolian genetic units by lava flows in the lower cretaceous of the Paraná Basin, southern Brazil. *Sedimentology*, **49**, 97–116.

Scherer, C.M.S. and **Goldberg, K.** (2007) Palaeowind patterns during the latest Jurassic-earliest cretaceous in Gondwana: evidence from aeolian cross-strata of the Botucatu formation, Brazil. *Palaeogeogr. Palaeoclimatol. Palaeoecol.*, **250**, 89–100.

Scherer, C.M.S. and **Lavina, E.L.C.** (2006) Stratigraphic evolution of a fluvial-eolian succession: the example of the upper Jurassic-lower cretaceous Guará and Botucatu formations, Paraná Basin, southernmost Brazil. *Gondw. Res.*, **9**, 475–484.

Shozaki, H. and **Hasegawa, H.** (2021) Development of longitudinal dunes under Pangaean atmospheric circulation. *Clim. Past*, **18**, 1529–1539.

Silva, F.G. and **Scherer, C.M.S.** (2000) Fácies, Associação de Fácies e Modelo Deposicional dos Arenitos Eólios da Formação Botucatu (Cretáceo Inferior) na Região Sul de Santa Catarina. *Pesqui. Em Geociências*, **27**, 15.

Sneh, A. and **Weissbrod, T.** (1983) Size-frequency distribution of longitudinal dune rippled flank sands compared to that of slipface sands of various dune types. *Sedimentology*, **30**, 717–725.

Swanson, T., **Mohrig, D.** and **Kocurek, G.** (2016) Aeolian dune sediment flux variability over an annual cycle of wind. *Sedimentology*, **63**, 1753–1764.

Swanson, T., **Mohrig, D.**, **Kocurek, G.** and **Liang, M.** (2017) A surface model for Aeolian dune topography. *Math. Geosci.*, **49**, 635–655.

Swanson, T., **Mohrig, D.**, **Kocurek, G.**, **Cardenas, B.T.** and **Wolinsky, M.A.** (2019) Preservation of autogenic processes and allogenic forcings in set-scale aeolian architecture I: numerical experiments. *J. Sediment. Res.*, **89**, 728–740.

Sweet, M.L., **Nielson, J.**, **Havholm, K.** and **Farrelley, J.** (1988) Algodones dune field of southeastern California: case history of a migrating modern dune field. *Sedimentology*, **35**, 939–952.

Thiede, D.S. and **Vasconcelos, P.M.** (2010) Paraná flood basalts: rapid extrusion hypothesis confirmed by new 40Ar/39Ar results. *Geology*, **38**, 747–750.

Thomas, D.S.G. (1988) Analysis of linear dune sediment-form relationships in the Kalahari dune desert. *Earth Surf. Process. Landf.*, **13**, 545–553.

Tsoar, H. (1978) The dynamics of longitudinal dunes. Ben-Gurion Univ Of The Negev Beersheba (Israel) Dept Of Geography, Beersheba.

Vermeesch, P. (2013) Multi-sample comparison of detrital age distributions. *Chem. Geol.*, **341**, 140–146.

Vermeesch, P. and **Garzanti, E.** (2015) Making geological sense of "big data" in sedimentary provenance analysis. *Chem. Geol.*, **409**, 20–27.

Waichel, B.L., **de Lima, E.F.**, **Sommer, C.A.** and **Lubachesky, R.** (2007) Peperite formed by lava flows over sediments: an example from the Central Paraná continental flood basalts, Brazil. *J. Volcanol. Geotherm. Res.*, **159**, 343–354.

Waichel, B.L., **Scherer, C.M.S.** and **Frank, H.T.** (2008) Basaltic lava flows covering active aeolian dunes in the Paraná Basin in southern Brazil: features and emplacement aspects. *J. Volcanol. Geotherm. Res.*, **171**, 59–72.

Wang, X., **Dong, Z.**, **Zhang, J.**, **Qu, J.** and **Zhao, A.** (2003) Grain size characteristics of dune sands in the central Taklimakan Sand Sea. *Sediment. Geol.*, **161**, 1–14.

Warren, A. (1972) Observations on dunes and bi-modal sands in the Ténéré Desert. *Sedimentology*, **19**, 37–44.

Wasson, R.J. (1983) Dune sediment types, sand colour, sediment provenance and hydrology in the Strzelecki-Simpson dunefield, Australia. *Eolian Sediment. Process*, **38**, 165–195.

Watson, A. (1986) Grain-size variations on a longitudinal dune and a barchan dune. *Sediment. Geol.*, **46**, 49–66.

Werner, B.T. (1995) Eolian dunes: computer simulations and attractor interpretation. *Geology*, **23**, 1107–1110.

Werner, B.T. (1999) Complexity in natural landform patterns. *Science*, **284**, 102–104.

Wilson, I.G. (1973) Ergs. *Sediment. Geol.*, **10**, 77–106.

Wickham, H., **Averick, M.**, **Bryan, J.**, **Chang, W.**, **McGowan, L.D.**, **François, R.**, **Grolemund, G.**, **Hayes, A.**, **Henry, L.**, **Hester, J.**, **Kuhn, M.**, **Pedersen, T.L.**, **Miller, E.**, **Bache, S.M.**, **Müller, K.**, **Ooms, J.**, **Robinson, D.**, **Seidel, D.P.**, **Spinu, V.**, **Takahashi, K.**, **Vaughan, D.**, **Wilke, C.**, **Woo, K.** and **Yutani, H.** (2019) Welcome to the tidyverse. *J Open Source Softw.*, **4**, 1686.

Yu, X., **Liu, C.**, **Wang, C.** and **Wang, J.** (2021a) Late cretaceous aeolian desert system within the Mesozoic fold belt of South China: Palaeoclimatic changes and tectonic forcing of east Asian erg development and preservation. *Palaeogeogr. Palaeoclimatol. Palaeoecol.*, **567**, 110299.

Yu, X., **Wang, C.**, **Bertolini, G.**, **Liu, C.** and **Wang, J.** (2021b) Damp- to dry aeolian systems: sedimentology, climate forcing, and aeolian accumulation in the late cretaceous Liyou Basin, South China. *Sediment. Geol.*, **426**, 106030.

Zieger, J., **Harazim, S.**, **Hofmann, M.**, **Gärtner, A.**, **Gerdes, A.**, **Marko, L.** and **Linnemann, U.** (2020) Mesozoic deposits of SW Gondwana (Namibia): unravelling Gondwanan sedimentary dispersion drivers by detrital zircon. *Int J Earth Sci.*, **109**, 1683–1704.

Zhang, Z. and **Dong, Z.** (2015) Grain size characteristics in the Hexi Corridor Desert. *Aeolian Res.*, **18**, 55–67.

Zhou, N., **Li, Q.**, **Zhang, C.-L.**, **Chi-Hua, H.**, **Wu, Y.**, **Zhu, B.**, **Cen, S.** and **Huang, X.** (2021) Grain size characteristics of aeolian sands and their implications for the aeolian dynamics of dunefields within a river valley on the southern Tibet plateau: a case study from the Yarlung Zangbo river valley. *Catena*, **196**, 104794.

Manuscript received 28 June 2022; revision accepted 5 January 2023

Supporting Information

Additional information may be found in the online version of this article:

Appendix S1. Raw data including grain-size data, sample location, palaeowind data, provenance data.
Appendix S2. Rmarkdown scripts containing the study analysis.

